

RESEARCH ARTICLE

Optimizing PEEK impact strength through multi-objective FDM 3D printing

C. Padhy^{1*}, Suryakumar S.², D. Bhattacharjee³

¹ Department of Mechanical Engineering, Gandhi Institute of Technology and Management, 500081, Hyderabad, India

² Department of Mechanical and Aerospace Engineering, Indian Institute of Technology, 502284, Hyderabad, India

³ Department of Operations and Analytics, FLAME University, 412115, Pune, India

ABSTRACT - Thermoplastic materials such as Polylactic acid, Acrylonitrile Butadiene Styrene, Polyethylene terephthalate glycol, Nylon, and Thermoplastic polyurethane are favoured in Fused deposition modeling 3D printing due to their cost-effectiveness and versatile properties. However, with the introduction of high grade thermoplastic material poses compatibility challenges with existing machines and processes, impeding widespread adoption in FDM 3D printing. Incorporating new materials into 3D printing requires adjustments to hardware, software, and settings, leading to potential expenses and time investments. Maintaining quality control and consistency becomes complex as each material demands specific parameters and processing conditions. This variability hinders achieving consistent part quality in 3D printing. Moreover, achieving optimal FDM parameters for high-grade polymers (HGP) like Polyether ether ketone (PEEK) is a challenge due to the distinctive nature of the property, requiring specialized careful considerations during its optimization process. The considerable thermal gradient and heat distribution during printing can lead to residual stresses and deformations, significantly affecting the quality and, in particular, its impact strength. This article optimizes an industry grade 3D printing PEEK based on the limited number of process parameters, namely, build orientation, in-fill density and chamber temperature. Further, the research tries to derive a predictive model for Impact Strength (IS), which is an important consideration for the 3D printed object. In this article, along with the Impact Strength, Printing Time and Material Usage are also studied to find empirical evidence of association between these output variables or response variables. The result indicates that there is a positive significant correlation or association between them. When utilizing a specific parameter setup, the resulting IS of 86.5 kJ/m², a print time of 89 minutes, and a material usage of 3.26 grams are achieved. Notably, there is a measurable reduction of 9.18% in printing time and a 11.66% decrease in material usage when the print density is set to 100% to optimize impact strength. This optimization approach proves the use of composite desirability is a better approach where multiple objectives need to be achieved. The proposed regression model predicts the impact strength with coefficient of determination value more than 50%.

ARTICLE HISTORY

Received : 25th Aug. 2023

Revised : 04th Nov. 2023

Accepted : 24th Nov. 2023

Published : 26th Dec. 2023

KEYWORDS

Fused deposition modeling

Impact strength

Print time

High grade polymer

Composite desirability

Predictive modelling

1.0 INTRODUCTION

Additive manufacturing (AM) offers several advantages over conventional manufacturing, including design flexibility, near net shape production (NNSP), and reduced material usage. Among various AM methods, fused filament fabrication (FFF), also known as fused deposition modeling (FDM), has become popular due to its simplicity, affordability, and widespread applications in prototyping, engineering, and education [1, 2]. FDM's layer-by-layer approach using melted filament enables efficient object creation with minimal waste generation, making it superior in terms of system cost and build time. 3D printed objects produced through FDM provide designers with valuable insights into form, functionality, and fitness. Over the years, with advancements in the development of high-performance polymers (refer to Figure 1), achieving desirable mechanical properties through FDM has been relatively challenging and to assess the mechanical behaviour of 3D printed parts, especially for high-grade polymers like Polyether ether ketone (PEEK), Polyetherketoneketone (PEKK), and Polyethylenimine (PEI), which serve as metal replacements [3, 4], so mechanical testing of them is crucial. PEEK and its various forms have found widespread use in diverse biomedical treatments, including applications in dental implants, orthopedic procedures, and maxillofacial surgery. Additionally, its exceptional strength and durability have made it a popular choice for a wide array of industrial purposes [5]. By subjecting parts to various mechanical loads such as tension, compression, bending, or torsion, engineers can evaluate their structural integrity, strength, durability, and performance characteristics. This allows them to identify any weaknesses or limitations and make informed decisions to optimise designs accordingly. Numerous studies [6 – 8] have focused on optimizing FDM-AM process parameters, such as layer thickness, raster angle, print speed, nozzle temperature, infill patterns, and density, to enhance mechanical properties like tensile, compression, and flexural strengths, as well as overall part performance and durability. Understanding and improving these mechanical properties are essential for expanding the applications of 3D printed parts in various industries.

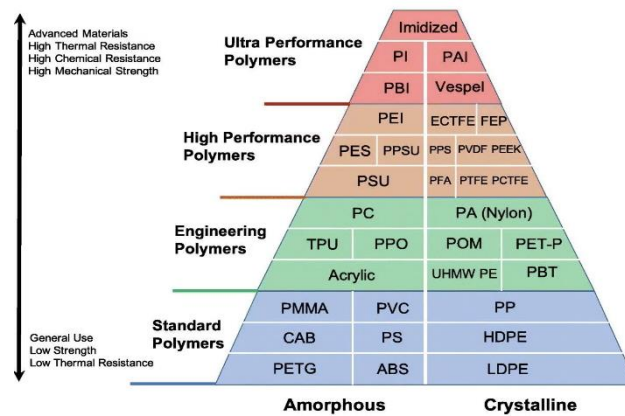


Figure 1. Classification of polymers [9]

The primary objective of this study is to evaluate the impact behavior of 3D-printed parts utilising high-performance polymers, with a particular emphasis on PEEK, a high-performance thermosetting polymer. Several past research studies have explored the influence of various process parameters on 3D printed PEEK parts, but limited attention has been given to the relationship between process parameters, build time, and its impact strength. For example, Zhang et al. (2004) studied the tribological properties of PEEK composites and explored the influence of filler content on mechanical characteristics to improve wear resistance in these composites [10]. Wu et al. (2014) analysed printing parameters impact on dimensional accuracy and thermal deformation in 3D printed PEEK, revealing that the printing process achieved good accuracy, but was found to be vulnerable to deformation under high-temperature [11]. Yang et al. (2017) investigated how thermal processing conditions influenced PEEK's crystallinity and mechanical properties, with higher printing and chamber temperatures promoting crystallinity and strength, while slower cooling rates improved crystallisation and mechanical performance [12]. Berretta et al. (2017) evaluated mechanical properties and thermal behaviour of CNT-PEEK composites fabricated using FDM, finding that incorporating carbon nano tubes (CNTs) improved mechanical properties but reduced thermal stability compared to pure PEEK [13]. Rinaldi et al. (2018) demonstrated that printing parameters significantly affected the mechanical strength of 3D printed PEEK parts, with layer height and raster angle negatively impacting strength, while higher printing temperatures improved mechanical properties [14]. Deng et al. (2018) explored optimal printing parameters to enhance PEEK's mechanical properties through FDM, including temperature, speed, and infill density [15]. Arif et al. (2018) studied biocompatible PEEK properties, analysing print orientation, layer thickness, and post-processing effects on mechanical behaviour and surface quality [16]. Later, in 2019 Saja et al. investigated PEEK for its potential as a denture material, with a specific focus on its mechanical properties [17]. Wang et al. (2019) observed that higher printing temperatures and lower printing speeds improved surface quality in PEEK, while excessive temperatures caused defects and degradation [18]. During the same time Li et al. (2019) investigated the flexural properties and fracture behaviour of CF/PEEK composites, analysing the effects of building orientation, fibre content, and fibre length [19]. Also, Yingshuang et al. (2019) claimed that adding multi-walled carbon nanotubes (MWCNTs) improved PEEK impact strength [20]. Moreover, the study conducted by Haijun, et al. in 2019 explored the impact strength of 3D printed PEEK, mainly on the evaluation of PEEK's resistance to impact forces, which further offering insights to its mechanical performance and suggested useful potential applications [21]. The work by Singh et al. (2019) explored the use of 3D printing technology to manufacture PEEK components for various biomedical applications, providing effective insights into the field of medicine and healthcare [22]. Zheng et al. (2021) fabricated PEEK/HA composite filaments, revealing an increase in tensile modulus but a decrease in tensile strength compared to pure PEEK [23]. Despite the existing research, very few studies have specifically investigated the relationship between process parameters, build time, and impact strength for high-performance polymers within 3D printing arena. Understanding and measuring optimum material impact strength are crucial for assessing safety, efficient and quality control in manufacturing processes.

Therefore, this research aims to assess the impact behaviour of 3D printed parts and examine the influence of process parameters, particularly print orientation, infill density, environmental condition-chamber temperature on impact strength while considering material usage and production efficiency. The article's organisation includes an introduction to the FDM process with PEEK and relevant research on process parameter optimization. Subsequent sections cover experimental details, methodology, comprehensive data analysis, and discussions of the important findings, and then concluding the research.

2.0 EXPERIMENTAL DETAILS

Figure 2 shows the schematic layout of FDM 3D PEEK printing, where CreatBot F160 PEEK-3D printer (manufacturer: Createbot Inc, China) is used to create the specimens. The 3D printer is equipped with a sizable build volume of (x:160mm, y:160mm, z:200mm) and incorporates a specialised heating system optimised for handling high-grade polymers efficiently.

2.1 Setting Parameters

Given the constraints of the research scope, the authors focused on the most critical printing parameters that directly impact the impact strength of thermoplastic polymers. These parameters were carefully selected based on insights gleaned from various previous studies. For the investigation, the author chose to work with PEEK, a high-grade polymer featuring a filament diameter of 1.75 mm. Table 1 outlines the essential properties of PEEK. By systematically studying the influence of specific printing parameters on PEEK's mechanical properties, the aim was to gain valuable insights into enhancing the impact strength of 3D printed PEEK components.

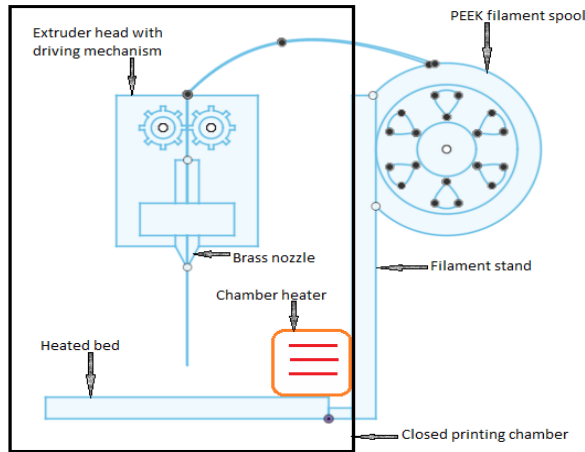


Figure 2. Schematic layout of FFF 3D PEEK printing

2.2 Sample Preparation

A nano polymer adhesive (manufacturer: Visionminer) designed for high-temperature build plate glue was initially used to address the common issue of bottom layer stick-out encountered while handling PEEK in Fused Deposition Modeling (FDM-AM). To further enhance print quality and reduce defects caused by moisture in the PEEK filament, the filament was dried in a filament drier (manufacturer: Creality Inc.) for 2 hours at 60°C, following the recommendations from Cicala et al. (2017) [24]. For the experiment, SolidWorks (2022 edition) was employed to model the printed samples according to ASTM standards (refer to Figure 3). The STL file (*.stl) of the samples was then imported into Simplify3D, a licensed 3D slicing software, to configure print parameters and generate the necessary G-Code for the 3D-printer. To optimise the impact strength (IS) of PEEK, the study considered various print parameters, such as chamber temperature (CT) and build orientation (XY: horizontal, XZ: vertical, refer to Figure 4(a) and (b)). Specimens were printed using the optimised parameters for strength [25] which included a layer thickness of 0.01 mm, nozzle temperature of 440 °C, print direction at 0°, while printed with a speed of 15 mm/sec and 0.4 mm brass nozzle [25]. The bed temperature was maintained at 120 °C for printing all specimens used in this research. The impact of print density, along with other selected print parameters on the impact strength of PEEK was investigated through the fabrication of the specimens (refer to Figure 4(c)). Moreover, balancing the strength, weight, and print time, the optimal infill density was determined through iterative testing and adjustments.

Table 1. Properties of PEEK [3]

Properties	Values	Properties	Values
Specific gravity	1.3 gm/cc	Flexural strength	125-128 MPa
Glass transition temperature	143 °C	Young's modulus	3.7 GPa
Melting point	340 °C	Operating temperature	250 °C

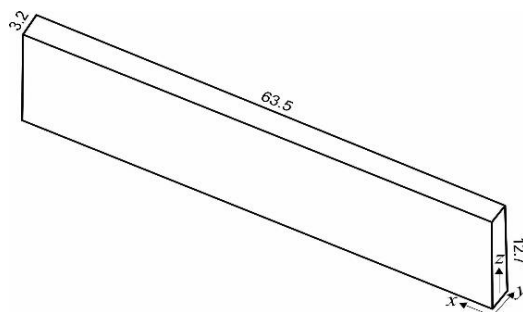


Figure 3. CAD model of the specimen (all dimensions are in mm)

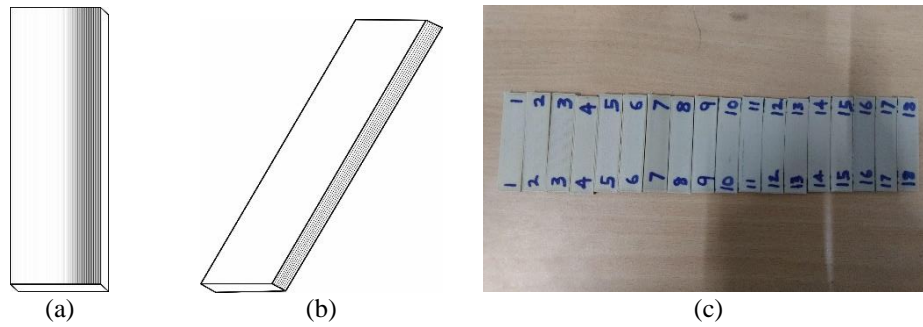


Figure 4. Representation of: (a) XY-build orientation, (b) XZ-build orientation and (c) Printed impact test specimens

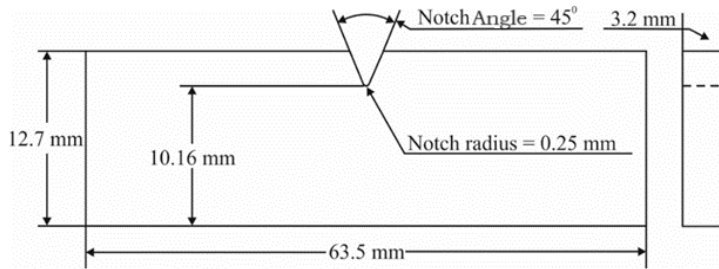


Figure 5. Specification of notched ASTM D256 specimen

2.3 Sample Testing

Subsequently, the printed specimens were notched in accordance with the ASTM standard (see Figure 5) and prepared for the mechanical Izod impact test (see Figure 6). The Izod impact test was conducted using an Izod impact tester (manufacturer: Deepak Polyplast, Unique ID No.: KL/ICT/01, Sl. No.: 2K103074) equipped with a digital impact indicator and a hammer mass of 4260 gms (see Figure 7).

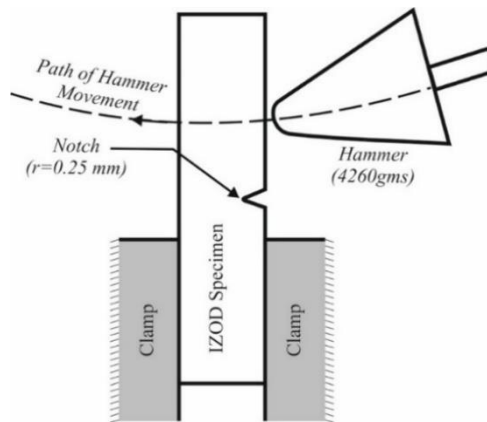


Figure 6. Impact test of ASTM D256 specimen



Figure 7. Izod impact test equipment

3.0 METHODOLOGY

The optimization of the 3D printing process involves systematically selecting appropriate process parameter values to achieve specific objectives, where the desired response variable or performance parameter is maximized or minimized. In simpler terms, it's about finding the best combination of settings to achieve the desired outcome in the 3D printed object. In this PEEK material based printing process parameters, namely, print orientation (PO), print density (PDN) and chamber temperature (CT) [in °C] are considered. In extrusion based 3D printing process, the mentioned process parameters are highly discussed in the earlier published articles as mentioned in the introduction section. Now, three response variable or performance variables, namely, print time (PT) [in mins], impact strength (IS) [in kJ/m²] and material used (MU) [in gms] are considered in this article. In the manufacturing sector, production time is a vital parameter to measure the efficiency of the manufacturing process along with the product quality. On the other hand, in case of 3D printing process, impact strength is one of the important parameters for measuring the print quality. Along with these response parameters, material utilization indicator related to printing cost, is also considered as one of the important response variable. This research initially uses analysis of variance (ANOVA) method for finding the individual process parameters impact on the selected response variable. Next correlation analysis has been used to know the association between the process parameters and the response variables. The ANOVA and Correlation analysis indicates a proper explanation of the relationship between them. Then two different modified Taguchi methods, namely, Taguchi and Composite Desirability Taguchi (TOPSIS), are used to optimize the method and the final results are compared with mix Taguchi method for result comparison and at the end a Regression equation is derived for estimating the impact strength of printed object for PEEK.

3.1 Data Generation

The initial data generation has been done through conducting lab experiments. In this article the data for the analysis has been generated based on the orthogonal array L18, which is a schema for performing experiments [26]. Here the L18 orthogonal array is selected as the number of process parameters are three with a mixed number of levels. The detailed level information for various input parameters including output parameters used in this article has been provided in Table 2. Also the parameters, which are kept constant during the printing process, are provided in the same Table 2.

Table 2. Details of printing parameters

Input Parameter(s)	Level			Output Parameter(s)
Level (s)	Level 1	Level 2	Level 3	
Print Orientation (PO)	XY	XZ	-	Impact Strength (IS)
Print Density (PDN)	High (100%)	Medium (90%)	Low (80%)	Print Time (PT)
Chamber Temperature (CT)	70° C	60° C	50° C	Material Utilization (MU)
Other setting print parameters, which are kept constant				
Nozzle temperature	440 °C	Print speed	15 mm/sec	
Layer height	0.01 mm	Print direction	0°	

The orthogonal array with the response values is provided in Table 3. In this table aforementioned three process parameters levels along with the response values, which are obtained through lab testing are provided. This data set is further used for all kind of data analysis process for performing correlation analysis, analysis of variance, process optimization and regression analysis.

Table 3. L18 OA data for analysis

TN	PO	PDN (%)	CT (°C)	PT (mins)	IS (kJ/m ²)	MU (gms)
1	XY	80	50	84	74.03	3.08
2	XY	80	60	84	75.51	3.08
3	XY	80	70	84	75.88	3.08
4	XY	90	50	89	117.59	3.27
5	XY	90	60	89	91.33	3.27
6	XY	90	70	89	100.51	3.27
7	XY	100	50	98	112.48	3.64
8	XY	100	60	98	81.61	3.64
9	XY	100	70	98	96.53	3.64
10	XZ	80	50	84	65.25	3.08
11	XZ	80	60	84	71.79	3.08
12	XZ	80	70	84	55.98	3.08

Table 3. (cont.)

TN	PO	PDN (%)	CT (°C)	PT (mins)	IS (kJ/m ²)	MU (gms)
13	XZ	90	50	89	86.98	3.27
14	XZ	90	60	89	72.63	3.27
15	XZ	90	70	89	99.78	3.27
16	XZ	100	50	98	230.4	3.64
17	XZ	100	60	98	224.13	3.64
18	XZ	100	70	98	225.49	3.64

*TN=Treatment No.

3.2 Analysis of variance (ANOVA)

Analysis of variance is a process where the variances in response variables are analyzed to understand the contribution of each process parameter. The ANOVA has been conducted for each response variable and tabulated the summary of the analysis in Tables 4 through 6 [26]. The important statistics can be found in the table which are useful for describing the phenomenon.

Table 4. Analysis of variance for impact strength

Source	df	Adj SS	Adj MS	F Value	P Value	VIF
Regression	3	30733.4	10244.5	6.06	0.007	
PDN	1	25410.4	25410.4	15.04	0.002	1
CT	1	88.3	88.3	0.05	0.822	1
PO	1	5234.7	5234.7	3.10	0.100	1
Error	14	23648.2	1689.2			
Total	17	54381.6				

Table 5. Analysis of variance for print time

Source	df	Adj SS	Adj MS	F	p	VIF
Regression	3	588.0	196.000	171.50	0.00	
PDN	1	588.0	588.000	514.50	0.00	1
CT	1	0.0	0.000	0.00	1.00	1
PO	1	0.0	0.000	0.00	1.00	1
Error	14	16.0	1.143			
Total	17	604.0				

Table 6. Analysis of variance for material used

Source	df	Adj SS	Adj MS	F	p	VIF
Regression	3	0.9408	0.3136	135.51	0.00	
PDN	1	0.9408	0.9408	406.52	0.00	1
CT	1	0.000	0.0000	0.00	1.00	1
PO	1	0.000	0.0000	0.00	1.00	1
Error	14	0.0324	0.002314			
Total	17	0.9732				

According to the Tables 4 through 6, the contribution of PDN in variance for all response variables is highest. In case of impact strength, the second highest contributor in variance is print orientation (PO). Similarly based on the F value and p value it can be stated that the (PDN) has a significant impact on the response variables.

3.3 Pearson Correlation

A correlation analysis has been conducted to know the association between different types of variables before process optimization. Pearson correlation is a method for finding the statistical association between two variables. This basically is the ratio of covariance and product of standard deviation. The correlation coefficient provides useful information how the two variables behaves to each other according to the collected data. The expression for calculating the Pearson correlation coefficient (r_p) is provided in Eq. (1) [27]. The calculated correlation coefficients are provided in Table 7.

$$r_p = \frac{\sigma_{x,y}}{\sigma_x \sigma_y} \tag{1}$$

where, $\sigma_{x,y}$ is indicating the covariance of two variables x and y, σ_x and σ_y are the standard deviation of x and y.

Table 7. Correlation analysis summary

	PDN	CT	PT	IS	MU
PDN	1.000				
CT	0.000	1.000			
PT	0.987**	0.000	1.000		
IS	0.684**	-0.040	0.704**	1.000	
MU	0.983**	0.000	1.000**	0.705**	1.000

** indicates the 95% confidence interval

According to the data, material utilization (MU) and print time (PT) has full positive significant correlation. Similarly, impact strength (IS) and MU have high significant positive correlation (0.705**). The impact strength is high positively correlated to print time (0.704**). As per the correlation values, if only material utilization is considered in analysis then the print time will be automatically taken care off. So, accordingly further in the optimization of process only MU and IS are considered. The correlation analysis also indicates that which process parameters out of the selected three process parameter need to be given importance while optimizing the process. The correlation analysis indicates the print density have high positive correlation on the IS, MU and PT. So, print density is an important parameter while optimizing the process in the present scenario.

3.4 Taguchi’s Design of Experiment

Taguchi’s design of experiment (DOE) is an optimization method, which considers the impact of the levels of the process parameters on the response value. This method is a very popular method of optimization as it considers the loss function for finding the right combination of process parameter levels to generate the optimal value of response. The two concepts for such optimization are Smaller-the-better and Larger-the-better. The signal to noise ratio for smaller the better (SNR_s) and larger the better (SNR_L) calculations for the two cases are represented with Eqs. (2) and (3) [26].

$$SNR_s = -10 \log \log \left(\frac{1}{n} \sum_{i=1}^n y_i^2 \right) \tag{2}$$

$$SNR_L = -10 \log \log \left(\frac{1}{n} \sum_{i=1}^n \frac{1}{y_i^2} \right) \tag{3}$$

The Taguchi method is applied to optimize individual response variables. The main effect and signal to noise effect has been observed and the effects are provided in Tables 8 through 10.

Table 8. Main effect of signal to noise ratio and mean value for impact strength

Levels	Signal to noise ratio			Mean		
	PO	PDN	CT	PO	PDN	CT
1	39.13	36.82	40.36	91.72	69.74	114.46
2	40.63	39.44	39.39	125.83	94.80	102.83
3		43.38	39.89		161.77	109.03
Delta	1.50	6.56	0.96	34.11	92.03	11.62
Rank	2	1	3	2	1	3

Table 9. Main effect of signal to noise ratio and mean value for print time

Levels	Signal to noise ratio			Mean		
	PO	PDN	CT	PO	PDN	CT
1	-39.10	-38.49	-39.10	90.33	84.00	90.33
2	-39.10	-38.99	-39.10	90.33	89.00	90.33
3		-39.82	-39.10		98.00	90.33
Delta	0.00	1.34	0.000	0.000	14.00	0.000
Rank	2.5	1	2.5	2.5	1	2.5

Table 10. Main effect of signal to noise ratio and mean value material used

Levels	Signal to noise (S/N) ratio			Mean		
	PO	PDN	CT	PO	PDN	CT
1	-10.428	-9.771	-10.428	3.330	3.080	3.330
2	-10.428	-10.291	-10.428	3.330	3.270	3.330
3		-11.222	-10.428		3.640	3.330
Delta	0.000	1.451	0.000	0.000	0.560	0.000
Rank	2.5	1	2.5	2.5	1	2.5

The data is analysed using the Taguchi DOE for the objective of smaller the better. Here for the three response parameters data analysis has been presented in Tables 6 through 8. In Table 6, 7, and 8 the main effect of signal to noise ratio (S/N) and mean can be observed where the PDN got the highest rank of 1. On the other hand, PO and CT have an equal rank of 2.5 for PT and MU. While, in case of IS, the PO has got rank 2 and CT ranked as 3.

3.5 Technique for Order Preference by TOPSIS based Taguchi

Technique for TOPSIS is a method for selecting the best alternative based on the criteria values [28]. The technique is a well-known multicriteria decision making method and this method is utilized for combining the three response variables into a single variable for applying the Taguchi based response optimization.

Step 1: Prepare the table containing the alternatives and criteria values (x_{ij}). Fix the weight values (w_{ij}) for the criterias.

Step 2: Normalise the criteria values for particular alternatives using Eq. (4).

$$r_{ij} = \frac{x_{ij}}{\sqrt{\sum_{k=1}^m x_{kj}^2}} \quad i = 1,2,3, \dots, n; j = 1,2,3 \dots, m \tag{4}$$

where n is the number of alternatives and m is the number of criteria.

Step 3: Calculate the weighted normalised values (v_{ij}) for criteria for alternatives based on the Eq. (5).

$$v_{ij} = r_{ij} \times w_{ij} \tag{5}$$

Step 4: Identify the positive ideal solution (A^+) and negative ideal solution (A^-) which are represented with Eqs. (6) and (7).

$$A^+ = \{v_1^+, v_2^+, \dots, v_m^+\} \tag{6}$$

$$A^- = \{v_1^-, v_2^-, \dots, v_m^-\} \tag{7}$$

Step 5: Calculate the distance (d_{pi}) between every alternative and positive ideal solution using Eq. (8). Similarly, calculate the distance (d_{ni}) between every alternative and negative ideal solution using Eq. (9).

$$d_{pi} = \sqrt{\sum_{j=1}^m (v_{ij} - v_j^+)^2} \tag{8}$$

$$d_{ni} = \sqrt{\sum_{j=1}^m (v_{ij} - v_j^-)^2} \tag{9}$$

Step 6: Now calculate (C^*) using Eq. (10). The range of value for $0 \leq C^* \leq 1$

$$C^* = \frac{d_{ni}}{d_{pi} + d_{ni}} \tag{10}$$

Here, the lower value of C^* is desired as it indicates a solution nearer to the positive ideal solution. In the proposed methodology this C^* is used as the response variable for Taguchi's design for experiment based optimization. Such an approach of hybridization, where a multicriteria decision making approach is combined with design of experiment can be found in recent literature [29, 30] for combining several objectives.

The 18-treatment condition can be considered as alternatives for the process of the TOPSIS method. The three response variables can be considered as the criteria for the best alternative selection. Two different sets of weight values are considered (0.4,0.3,0.3) and (0.5,0.25,0.25) for IS, PT and MU. The main reason for assigning same weight values to PT and MU is because of the full correlation between them ($r_p = 1.00^{**}$).The TOPSIS scores C^* for these two cases are

provided in Figure 8. The intermediate calculation of weighted normalised matrix, distance from positive ideal solution (d_{pi}), distance from negative idle solution (d_{ni}) and TOPSIS score C^* for each alternative has been provided for the two cases with different criteria weights in Table 11 and Table 13 given below. The ANOVA for the two TOPSIS scores are also provided in Table 12 and Table 14. This selection of best alternative using TOPSIS has been conducted for weight values of IS, keeping the other two responses with equal weightage indicates no change in best alternative selection.

Table 11. Weighted normalized alternatives for TOPSIS case 1

Alternatives	W_{IS}	W_{PT}	W_{MU}	d_{pi}	d_{ni}	C^*
	0.4	0.3	0.3			
	nIS*w	nPT*w	nMU*w			
1	0.057270408	0.065618325	0.065243	0.12096952	0.021338	0.850057801
2	0.058415352	0.065618325	0.065243	0.11982458	0.022104	0.844259063
3	0.058701588	0.065618325	0.065243	0.11953834	0.022301	0.842774403
4	0.090968894	0.069524178	0.069268	0.08745106	0.048811	0.641784616
5	0.070653874	0.069524178	0.069268	0.10773214	0.029304	0.786158688
6	0.077755622	0.069524178	0.069268	0.1006407	0.036022	0.736416829
7	0.087015743	0.076554713	0.077106	0.09264002	0.043709	0.67943292
8	0.063134377	0.076554713	0.077106	0.11623084	0.019828	0.854271166
9	0.074676651	0.076554713	0.077106	0.10481256	0.03137	0.769647921
10	0.050478105	0.065618325	0.065243	0.12776182	0.017656	0.878581716
11	0.055537519	0.065618325	0.065243	0.12270241	0.020246	0.85836659
12	0.043306733	0.065618325	0.065243	0.1349332	0.016134	0.893197063
13	0.067288667	0.069524178	0.069268	0.11109292	0.026191	0.809217711
14	0.056187352	0.069524178	0.069268	0.12218136	0.016636	0.880156954
15	0.077190886	0.069524178	0.069268	0.10120456	0.035482	0.74041181
16	0.178239928	0.076554713	0.077106	0.01613447	0.134933	0.106802937
17	0.173389389	0.076554713	0.077106	0.01684782	0.130083	0.114665222
18	0.174441499	0.076554713	0.077106	0.01657556	0.131135	0.112216665

**Note: PIS: [0.065618325,0.178239928,0.065243]; NIS: [0.076554713,0.043306733,0.077106]
 W indicates the weight value for particular response variable, n indicates the normalized value.

Table 12. Analysis of variance for first case 1

Source (TS1)	df	Adj SS	Adj MS	F	p	VIF
Regression	3	1.03829	0.346096	6.59	0.005	
PDN	1	0.87513	0.875135	16.67	0.001	1.00
CT	1	0.00267	0.002668	0.05	0.825	1.00
PO	1	0.16048	0.160484	3.06	0.102	1.00
Error	14	0.73500	0.052500			
Total	17	1.77328				

Table 13. Weighted normalised alternatives for TOPSIS case 2

Alternatives	W_{IS}	W_{PT}	W_{MU}	d_{pi}	d_{ni}	C^*
	0.5	0.25	0.25			
	nIS*w	nPT*w	nMU*w			
1	0.071588009	0.054681938	0.054369	0.15199633	0.036056	0.808267094
2	0.073019189	0.054681938	0.054369	0.15057261	0.03677	0.803728824
3	0.073376984	0.054681938	0.054369	0.1502167	0.036955	0.802561012
4	0.113711117	0.057936815	0.057723	0.10961715	0.065359	0.626468983
5	0.088317343	0.057936815	0.057723	0.13491151	0.043484	0.756250303
6	0.097194527	0.057936815	0.057723	0.12606454	0.05076	0.71293648
7	0.108769679	0.063795594	0.064255	0.11404908	0.057559	0.664589572
8	0.078917972	0.063795594	0.064255	0.14389688	0.030696	0.824187466
9	0.093345813	0.063795594	0.064255	0.1294707	0.043192	0.749847293
10	0.063097631	0.054681938	0.054369	0.1604452	0.032798	0.83027575
11	0.069421899	0.054681938	0.054369	0.15415142	0.035058	0.814711362
12	0.054133416	0.054681938	0.054369	0.1693701	0.031549	0.842975485
13	0.084110834	0.057936815	0.057723	0.13910505	0.040261	0.775537348
14	0.070234191	0.057936815	0.057723	0.15294396	0.031329	0.829983818
15	0.096488607	0.057936815	0.057723	0.1267679	0.050162	0.716485118
16	0.22279991	0.063795594	0.064255	0.00207354	0.169636	0.012075839
17	0.216736736	0.063795594	0.064255	0.00640794	0.163609	0.037690066
18	0.218051874	0.063795594	0.064255	0.00518106	0.164916	0.030459486

**Note PIS: [0.054681938, 0.22279991, 0.054369]; NIS: [0.063795594, 0.054133416, 0.064255],
W indicates the weight value for particular response variable, n indicates the normalized value.

Table 14. Analysis of variance for case 2

Source (TS2)	df	Adj SS	Adj MS	F	p	VIF
Regression	3	0.471945	0.157315	6.69	0.005	
PDN	1	0.436419	0.436419	18.55	0.001	1.00
CT	1	0.002183	0.002183	0.09	0.765	1.00
PO	1	0.033344	0.033344	1.42	0.254	1.00
Error	14	0.329298	0.023521			
Total	17	0.801243				

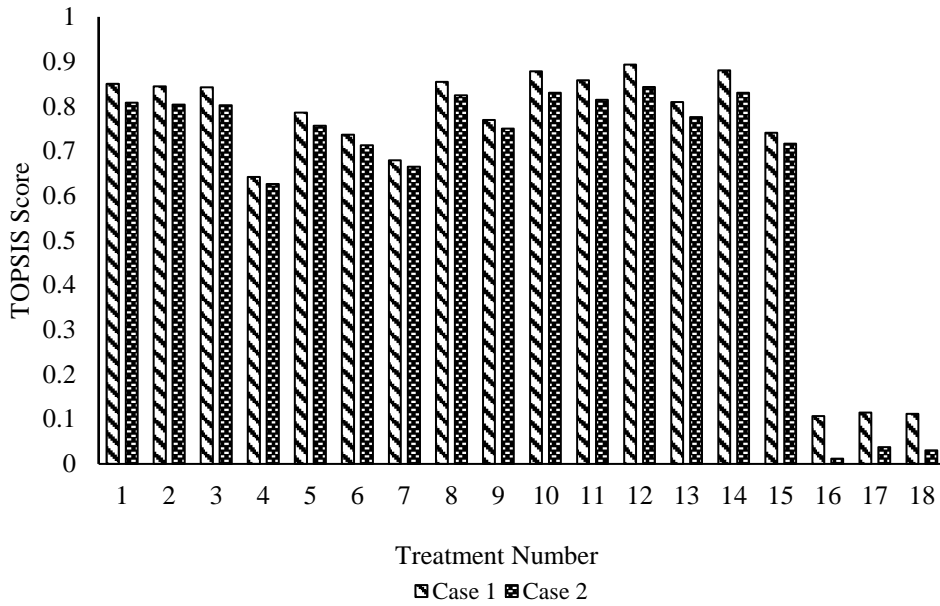


Figure 8. Weighted normalised alternatives for TOPSIS score for two cases

The application of the Taguchi based method on the TOPSIS scores for two cases indicates that the importance of PDN is highest followed by PO and CT. The main effects of signal to noise ratio and mean for both cases are provided in Table 15 and Table 16. The delta values and rank for all process parameters are provided in same tables. The score of C* is used as the response variable for Taguchi design experiment with smaller-the-better approaches. The calculated levels for the three process parameters are PDN=100%, PO=XZ and CT=50°C. The details for the results has been provided in results discussion. So further, the same problem has been solved using composite desirability.

Table 15. Main effect of signal to noise ratios and mean for case 1

Levels	Signal to Noise ratio			Mean		
	PO	PDN	CT	PO	PDN	CT
1	2.218	1.300	5.169	0.7783	0.8612	0.6610
2	7.359	2.360	4.363	0.5993	0.7657	0.7230
3		10.706	4.835		0.4395	0.6824
Delta	5.140	9.406	0.806	0.18885	0.4217	0.0620
Rank	2	1	3	PO	PDN	CT

Table 16. Main effect of signal to noise ratios and mean for case 2 (Smaller is the better)

Levels	Signal to Noise ratio			Mean		
	PO	PDN	CT	PO	PDN	CT
1	2.132	1.047	5.602	0.7867	0.8867	0.6655
2	8.229	2.291	4.720	0.6009	0.7720	0.7284
3		12.203	5.220		0.4228	0.6875
Delta	6.098	11.155	0.883	0.1858	0.4639	0.0629
Rank	2	1	3	2	1	3

3.6 Composite Desirability Based Optimization

The traditional Taguchi analysis can provide the optimal process parameter value for a specific objective, but it has limitation in tackling multiple objectives. Now here two objectives, namely, maximum impact strength and minimum material utilization is considered as there two parameters for optimization problem. The composite desirability, D is calculated based on the Eqs. (11) through (13) [31], whereas desirability function $d_j(Y_j)$ is used to converts the response values $Y_j(x)$, between 0 and 1. The individual desirability values are combined using Eq. (11), which gives the composite desirability, D.

$$D = (d_1(Y_1) \times d_1(Y_1) \times \dots \times d_k(Y_k))^{1/k} \tag{11}$$

where, ‘k’ is the number of responses. The desirability for maximization is presented in Eq. (12).

$$d_j(Y_j) = \begin{cases} 0 & \text{if } Y_j < L_j \\ \left(\frac{Y_j - L_j}{T_j - L_j}\right)^s & \text{if } L_j \leq Y_j \leq T_j \\ 1 & \text{if } Y_j > T_j \end{cases} \tag{12}$$

Desirability function for Y_j response minimization

$$d_j(Y_j) = \begin{cases} 1 & \text{if } Y_j < T_j \\ \left(\frac{Y_j - U_j}{T_j - U_j}\right)^t & \text{if } T_j \leq Y_j \leq U_j \\ 0 & \text{if } Y_j > U_j \end{cases} \tag{13}$$

where, $s = t = 1$, the desirability function increases linearity towards T_j , for $s < 1$, $t < 1$ function is convex; $s > 1$, $t > 1$ concave.

After calculating the composite desirability, the multivariate gradient decent algorithm has been deployed for optimizing the process [32]. The expression for calculation has been provided in Eq. (14). Repeat the process until it converges, where J is the cost function (here the composite desirability), θ_m is the m^{th} decision variable or here it is the process parameter, N is number of process parameters and α is learning rate.

$$\theta_m = \theta_m - \alpha \sum_{m=0}^N \frac{\partial}{\partial \theta_m} J(\theta_0, \theta_1, \dots, \theta_N) \tag{14}$$

The composite desirability change with individual objectives is provided in Figure 9. This indicates for satisfying the objectives the print density should be 87.68%, chamber temperature of 50°C and orientation of XZ.

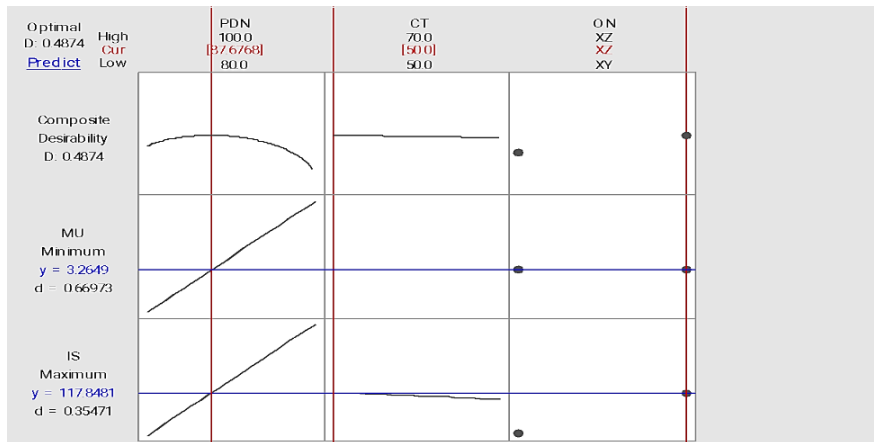


Figure 9. Desirability analysis summary

3.7 Regression Analysis

The Impact Strength estimation model is tried to derive with multiple combinations of process parameters. Regression method is deployed to establish the relationship between the impact strength and process parameters [33]. Here multiple regression models are created and then based on the Akaike Information Criterion (AIC) value [34], tries to find the best fit with minimum number fewest possible independent variable. The multiple fitted models are compared then based on minimum AIC best model is selected. The independent variable here is here impact strength and for improving the model multiple variables are created based on the concept of feature engineering. The variables are ON, PDN, CT, PDN x CT, PDN², CT². The tested models along with AIC values are provided in Table 17 and a model summary has been provided in Table 18.

Table 17. Model selection for estimating the impact strength

Model	Variable set	AIC
1	ON; PDN; CT; PDN x CT; PDN ² ; CT ²	141.58
2	ON; PDN; CT; PDN ² ;CT ²	139.60
3	ON; PDN; CT; PDN ²	137.86
4	ON; PDN; PDN ²	135.94
5	ON; PDN ²	135.01

Table 18. The summary of selected impact strength estimation model

	Coefficient	P value	Adjusted R ²
Intercept	-118.6045	0.0418	51.37%
ON: XZ	34.1067	0.0865	
PDN ²	0.0258	0.0010	

The selected predictive model has adjusted R² of 51.37%. It is indicating that the model parameters ON and PDN² can explain the 51.37% variability within the impact strength. The P value indicates that the PDN² have a significant impact on the Impact strength value. Thus, the regression model has been provided as Eq. (15).

$$\text{Impact Strength}_{XZ=1} = -118.6045 + 34.1067XZ + 0.0258PDN^2 \quad (15)$$

4.0 RESULTS AND DISCUSSION

The correlation coefficient values, and ANOVA indicates that the PDN has highest significance on the three response variables namely, Impact strength, Print time and Material utilization. Print density refers to the level of material filling within a 3D printed object [35]. Higher print density generally leads to increased material content and a more solid internal structure. As a result, higher PDN values can lead to improved impact strength of the printed parts. This is because a denser and more solid structure is less likely to crack or break upon impact compared to a part with lower print density, which may have voids or weaker regions [36]. However, it is important to note down that though the Print density affects the amount of material that needs to be deposited and solidified during the 3D printing process, higher PDN values often require more material to be printed, leading to longer print times. Conversely, lower print density can result in faster printing times as less material needs to be deposited. However, it's worth noting that the impact on print time may depend on other factors such as the printing technology, layer height, and complexity of the design etc. Material utilization refers to how efficiently the 3D printing process uses the input material to create the desired object. Higher print density implies more material is used, which may result in lower material utilization efficiency [36]. Conversely, lower PDN values may lead to better material utilization as less material is required to achieve the desired part geometry. Efficient material utilization is essential in reducing costs and minimizing waste in additive manufacturing [37-39]. Thus, it is important to note that the obtained relationship (refer to Eq. (15)) between PDN and the three response variables (impact strength, print time, and material utilization) may not be linear and also can vary further depending on the specific 3D printing technology and complexity of the object.

Though the Print time and Material utilization have perfect significant positive correlation and as per the observation from previous literatures the material used is directly related to print time [38, 39]. In case of three variables there is no as such any significant impact of independent variables chamber temperature and print orientation. It is important to note that Chamber temperature can play a crucial role in certain 3D printing processes, particularly in FDM when using temperature-sensitive materials like PEEK or when attempting to control the cooling rate of the printed parts [40, 41]. However, the controlled melting and solidification of the PEEK filament occurred through the careful consideration of nozzle temperature to ensure proper melting of the filament during extrusion [10,13,16]. The extruded material then quickly solidifies and fuses with the previously deposited layer. Since the melting and solidification occur in close succession, the chamber temperature might not have a substantial impact on the bonding process. Also, in addition to that the extruder head often follows overlapping paths during the printing process, resulting in the fusion of material between adjacent passes more frequently. This overlapping pattern promotes good bonding between layers, contributing to the overall strength of the 3D printed part and hence strength. Similarly, Print orientation refers to the way a 3D model is positioned on the build platform during printing. Different orientations can result in variations in mechanical properties, printing time, and material utilization [42, 43]. However, in some cases, the effect of print orientation on the response variables might not be significant, especially when other parameters like print density and layer height are well-optimized. The layer height and extrusion settings, such as nozzle temperature and extrusion rate, have a more significant influence on material bonding in FDM [41]. Properly optimizing these parameters can lead to strong interlayer adhesion and bonding, reducing the relative impact of chamber temperature and print orientation on material bonding [44].

In case of optimization three methods have been implemented for its analysis e.g., traditional Taguchi method, TOPSIS based Taguchi method and Composite desirability enabled gradient decent method. The optimization result indicates Taguchi based method fails to produce result out of the orthogonal array. But this method again indicates which

parameters are more influencing while going for optimization. It indicates print density with 100%, chamber temperature of 50°C and print orientation of XZ produces the highest impact strength but it requires higher print time of 98 min. Similar result also found in case of Taguchi based optimization where the target is maximization of impact strength. As the problem is a multi-objective problem, in that context the composite desirability produces moderate results. It selects the print density as 87.70%, chamber temperature of 50°C and print orientation of XZ. The solution indicates an impact strength value of 86.5 kJ/m², print time of 89 min and material utilization of 3.26 gm. The results from different methods are provided in Table 19. The reader can also refer to Table 20 for the main effect plot and signal to noise(S/N) ratio plot. Finally, the regression model proposed in Table 18 can be represented using Eq. (15), which can be used for estimating the impact strength of a 3D printed object printed with PEEK. The proposed predictive model is nonlinear or quadratic in nature and such model is very rare in the published domain.

Table 19. Objective wise selected process parameter value for optimal performance of the process

Method	Objective	PO	PDN (%)	CT (°C)	IS (kJ/m ²)	PT (min)	MU (gm)
Taguchi	Min PT	-	80	-	-	-	-
Taguchi	Max IS	XZ	100	50	230.4	98	3.64
Taguchi	Min MU	-	80	-	-	-	-
TOPSIS Taguchi	All Three	XZ	100	50	230.4	98	3.64
Composite Desirability with gradient decent method	All Three	XZ	87.70	50	86.5	89	3.26

Table 20. Main plot and S/N plot

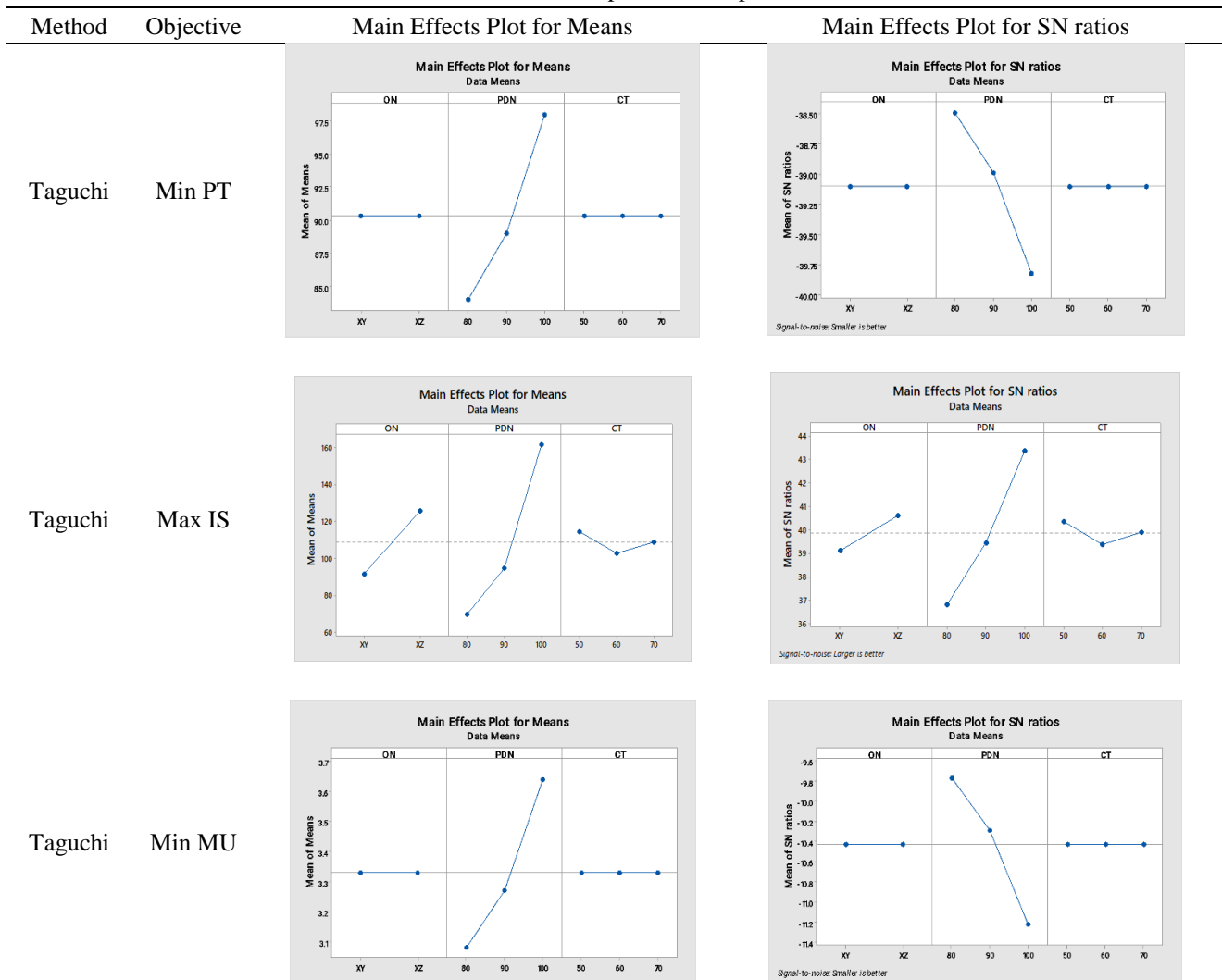


Table 20. (cont.)

Method	Objective	Main Effects Plot for Means	Main Effects Plot for SN ratios
TOPSIS Taguchi	All Three	<p>The plot shows the mean of means for three response variables (ON, PDN, CT) across two orientations (XY and XZ). The y-axis ranges from 0.4 to 0.9. For XY, the means are approximately 0.78 for ON and 0.60 for XZ. For PDN, the means are approximately 0.88 for ON and 0.45 for XZ. For CT, the means are approximately 0.68 for ON and 0.68 for XZ.</p>	<p>The plot shows the mean of SN ratios for three response variables (ON, PDN, CT) across two orientations (XY and XZ). The y-axis ranges from 0 to 12. For XY, the SN ratios are approximately 2.5 for ON and 7.5 for XZ. For PDN, the SN ratios are approximately 1.5 for ON and 10.5 for XZ. For CT, the SN ratios are approximately 5.5 for ON and 5.0 for XZ.</p>

5.0 CONCLUSIONS

The study concludes that higher print density or infill density enhances impact strength of a 3D printed object. However, this increases material usage and print time, which increase the manufacturing cost and time as well. PEEK is a costly printing material and hence, the consideration of material usage in the process optimization added an extra dimension to the problem. The printing time also considered along with the other two response variable for the same process. Finally, the objective of maximization of impact strength, minimization of material usage and minimization of printing time is considered for the process optimization. Different methods are deployed before process optimization to understand the relation between the process parameters and response variables. The correlation analysis and ANOVA indicates that the print density has significant impact on the three response variables. The print time and material usage have full positive significant correlation, which indicates there is a proportional relation between them. On the other side, the impact strength also has positive significant correlation with print time and material usage, which concludes while increasing the impact strength the material usage and printing time is higher. In case of process optimization, the three methods Taguchi, TOPSIS Taguchi and Composite desirability based gradient decent methods are deployed. Taguchi method fails to find the process parameters value for the objectives minimization of print time and material usage but selects the maximum print density of 100%, XZ as print orientation and 50°C of chamber temperature. Same process parameter values are selected with the TOPSIS based Taguchi method. The Impact strength obtained through is the 230.4 kJ/m², print time as 98 min and 3.64 gm of material usage. The proposed desirability coupled with gradient decent method selects print density as 87.70%, XZ as print orientation and 50°C of chamber temperature. This parameter setup produces Impact strength of 86.5 kJ/m², print time of 89 min, whereas 3.26 gm of Material usage, which is close to the treatment no. 13 from L18 OA (see Table 3). This definitely produces a printed object with comparable less impact strength but results in 9.18% less in printing time and 11.66 % of less material usage. Application wise, a minimum and a maximum value range for the impact strength and acceptable range for other response variables can be set for composite desirability coupled gradient decent method for obtaining desired results. Finally, the regression equation for predicting the impact strength has been proposed for the printed material in the XZ plane, which is useful for predicting the impact strength value.

6.0 ACKNOWLEDGMENTS

The authors express their sincere gratitude for the support provided by the Science and Engineering Research Board (SERB), Department of Science and Technology (DST), Government of India, through the Teachers Association for Research Excellence (TARE) scheme (Grant number: TAR/2020/000160).

7.0 REFERENCES

- [1] S. Vyavahare, S. Teraiya, D. Panghal and S. Kumar, "Fused deposition modelling: A review," *Rapid Prototyping Journal*, vol. 26, no. 1, pp.176-201, 2020.
- [2] L. Sandanamsamy, W. S. W. Harun, I. Ishak, F. R. M. Romlay, K. Kadirgama, D. Ramasamy, S. R. A. Idris and F. Tsumori, "A comprehensive review on fused deposition modelling of polylactic acid," *Progress in Additive Manufacturing*, vol. 8, pp. 775-799, 2023.
- [3] S. Sunpreet, P. Chander and R. Seeram, "3D printing of polyether-ether-ketone for biomedical applications," *European Polymer Journal*, vol. 114, pp. 234-248, 2019.
- [4] D. Arit, A. C. Camden, J. F. Jacob, E. Z. Callie, L. G. Eric, B. W. Christopher and J. B. Michael, "Current understanding and challenges in high temperature additive manufacturing of engineering thermoplastic polymers," *Additive Manufacturing*, vol. 34, p. 101218, 2020.
- [5] D. Garcia-Gonzalez, A. Rusinek, T. Jankowiak, and A. Arias, "Mechanical impact behavior of polyether-ether-ketone (PEEK)," *Composite Structures*, vol. 124, pp. 88-99, 2015.

- [6] K. Rajan, M. Samykano, K. Kadirgama, W. S. W. Harun, and M. M. Rahman, "Fused deposition modeling: Process, materials, parameters, properties, and applications," *International Journal of Advanced Manufacturing Technology*, vol. 120, no. 3-4, pp. 1531–1570, 2022.
- [7] H. Gonabadi, Y. Chen, A. Yadav, and S. Bull, "Investigation of the effect of raster angle, build orientation, and infill density on the elastic response of 3D printed parts using finite element microstructural modeling and homogenization techniques," *International Journal of Advanced Manufacturing Technology*, vol. 118, pp. 1485–1510, 2022.
- [8] A. Murali, M. A. Vakkattil and R. Parameswaran, "Investigating the effect of processing parameters on mechanical behavior of 3D fused deposition modeling printed polylactic acid," *Journal of Material Engineering and Performance*, vol. 32, pp. 1089–1102, 2023.
- [9] A. C. Christopher, Í. G. da Silva, K. D. Pangilinan, Q. Chen, E. B. Caldona and R. C. Advincula, "High performance polymers for oil and gas applications," *Reactive and Functional Polymers*, vol. 162, p. 104878, 2021.
- [10] Z. Zhang, C. Breidt, L. Chang and K. Friedrich, "Wear of PEEK composites related to their mechanical performances," *Tribology International*, vol. 37, no. 3, pp. 271-277, 2004.
- [11] W. Z. Wu, P. Geng, J. Zhao, Y. Zhang, D. W. Rosen and B. H. Zhang, "Manufacture and thermal deformation analysis of semicrystalline polymer polyether ether ketone by 3D printing," *Materials Research Innovations*, vol. 18, no. 5, pp. 12-16, 2014.
- [12] C. Yang, X. Tian, D. Li, Y. Cao, F. Zhao and C. Shi, "Influence of thermal processing conditions in 3D printing on the crystallinity and mechanical properties of PEEK material," *Journal of Materials Processing Technology*, vol. 248, pp. 1-7, 2017.
- [13] S. Berretta, R. Davies, Y.T. Shyng, Y. Wang and O. Ghita, "Fused deposition modelling of high temperature polymers: Exploring CNT PEEK composites," *Polymer Testing*, vol. 63, pp. 251-262, 2017.
- [14] M. Rinaldi, T. Ghidini, F. Cecchini, A. Brandao and F. Nanni, "Additive layer manufacturing of poly (ether ether ketone) via FDM," *Composites Part B*, vol. 145, pp. 162-172, 2018.
- [15] X. Deng, Z. Zeng, B. Peng, S. Yan and W. Ke, "Mechanical properties optimization of poly-ether-ether-ketone via fused deposition modeling," *Materials*, vol. 11, no. 2, pp. 216, 2018.
- [16] M. F. Arif, S. Kumar, K. M. Varadarajan and W. J. Cantwell, "Performance of biocompatible PEEK processed by fused deposition additive manufacturing," *Materials & Design*, vol. 146, pp. 249-259, 2018.
- [17] S. A. Muhsin, P. V. Hatton, A. Johnson, N. Sereno and D. J. Wood, "Determination of Polyetheretherketone (PEEK) mechanical properties as a denture material," *The Saudi Dental Journal*, vol. 31, no. 3, pp. 382-391, 2019.
- [18] P. Wang, B. Zou, H. Xiao, S. Ding and C. Huang, "Effects of printing parameters of fused deposition modeling on mechanical properties, surface quality, and microstructure of PEEK," *Journal of Materials Processing Technology*, vol. 271, pp. 62-74, 2019.
- [19] Q. Li, W. Zhao, Y. Li, W. Yang, and G. Wang, "Flexural properties and fracture behavior of CF/PEEK in orthogonal building orientation by FDM: Microstructure and mechanism," *Polymers*, vol. 11, no. 4, pp. 656, 2019.
- [20] S. Yingshuang, W. Xian, L. Yifan, J. Zilong, W. Zhaoyang, J. Zhenhua and Z. Haibo, "Preparation of PEEK/MWCNTs composites with excellent mechanical and tribological properties," *High Performance Polymers*, vol. 31, no. 1, pp. 43–50, 2019.
- [21] G. Haijun, X. Xiaodong and N. Jan, "Impact strength of 3D printed polyether-ether-ketone (PEEK)," in *Proceedings of the 30th Annual International Solid Freeform Fabrication Symposium—An Additive Manufacturing Conference*, Austin, Texas, USA, pp. 12–14, 2019.
- [22] S. Singh, C. Prakash and S. Ramakrishna, "3D printing of polyether-ether-ketone for biomedical applications," *European Polymer Journal*, vol. 114, pp. 234-248, 2019.
- [23] J. Zheng, J. Kang, C. Sun, C. Yang, L. Wang and D. Li, "Effects of printing path and material components on mechanical properties of 3D-printed polyether-ether-ketone/hydroxyapatite composites," *Journal of the Mechanical Behavior of Biomedical Materials*, vol. 118, p. 104475, 2021.
- [24] G. Cicala, A. Latteri, B. Del Curto, A. L. Russo, G. Recca and S. Farè, "Engineering thermoplastics for additive manufacturing: A critical perspective with experimental evidence to support functional applications," *Journal of Applied Biomaterials & Functional Materials*, vol. 15, pp. 10–18, 2017.
- [25] C. Padhy, S. Suryakumar, D. Bhattacharjee, R. Reddy, "Parametric analysis of 3D printing (FDM) process parameters on mechanical behaviour of PEEK- A high-grade polymer", *International Interdisciplinary Conference on Energy, Nanotechnology and Internet of Things*, ENT-2023, NIT-Puducherry, India, February 2-4, 2023.
- [26] D. C. Montgomery. Design and Analysis of Experiments, 10th Ed. *John Wiley & Sons Inc.*, 2019.
- [27] M. Ezekiel. Methods of Correlation Analysis, 2nd Ed. *John Wiley & Sons Inc.*, 1941.

- [28] B. Şimşek and T. Uygunoğlu, "Multi-response optimization of polymer blended concrete: A TOPSIS based Taguchi application." *Construction and Building Materials*, vol. 117, pp. 251-262, 2016.
- [29] D. Bhattacharjee, T. Ghosh, P. Bhola, K. Martinsen and P. Dan, "Ecodesigning and improving performance of plugin hybrid electric vehicle in rolling terrain through multi-criteria optimisation of powertrain," *Proceedings of the Institution of Mechanical Engineers, Part D: Journal of Automobile Engineering*, vol. 236, no. 5, pp. 1019-1039, 2022.
- [30] H. Korucu, B. Şimşek and A. Yartaşı, "A TOPSIS-based Taguchi design to investigate optimum mixture proportions of graphene oxide powder synthesized by hummers method," *Arabian Journal for Science and Engineering*, vol. 43, pp. 6033-6055, 2018.
- [31] N. R. Costa, J. Lourenço and Z. L. Pereira, "Desirability function approach: A review and performance evaluation in adverse conditions," *Chemometrics and Intelligent Laboratory Systems*, vol. 107, no. 2, pp. 234-244, 2011.
- [32] S. Ruder, "An overview of gradient descent optimization algorithms," *ArXiv*, vol, abs/1609.04747, 2016.
- [33] R. J. Freund, W. J. Wilson and P. Sa. Regression Analysis, 2nd Ed. *Academic Press*, 2006.
- [34] A. K. Seghouane, "New AIC corrected variants for multivariate linear regression model selection," *IEEE Transactions on Aerospace and Electronic Systems*, vol. 47, no. 2, pp. 1154-1165, 2011.
- [35] NWA3D, "Glossary of 3D Printing Terms," Accessed: August 2023, Available at <https://www.nwa3d.com/education/glossary-of-3d-printing-terms/>
- [36] J. Dobos, M. M. Hanon and I. Oldal, "Effect of infill density and pattern on the specific load capacity of FDM 3D-printed PLA multi-layer sandwich," *Journal of Polymer Engineering*, vol. 42, no. 2, pp. 118-128, 2022.
- [37] I. J. Petrick and T. W. Simpson "3D printing disrupts manufacturing: how economies of one create new rules of competition," *Research-Technology Management*, vol. 56, no. 6 pp. 12–16, 2013.
- [38] B. P. Conner, G. P. Manogharan, A. N. Martof, L. M. Rodomsky, C. M. Rodomsky, D. C. Jordan, and J. W. Limperos, "Making sense of 3-D printing: Creating a map of additive manufacturing products and services," *Additive Manufacturing*, vol. 1–4, pp. 64–76, 2014.
- [39] B. Liseli, M. Guha, M. Hazel, "Study of infill print design on production cost-time of 3D printed ABS parts," *International Journal of Rapid Manufacturing*, vol. 5, no. 3/4, pp. 308-319, 2015.
- [40] S. J. Park, J. E. Lee, J. Park, N. K. Lee, Y. Son and S. H. Park, "High-temperature 3D printing of polyetheretherketone products: Perspective on industrial manufacturing applications of super engineering plastics," *Materials & Design*, vol. 211, p. 110163, 2021.
- [41] R. Kumrai-Woodruff and Q. Wang, "Temperature control to increase inter-layer bonding strength in fused deposition modelling" *Proceeding of the ASME 2020 International Design Engineering Technical Conferences and Computers and Information in Engineering Conference*, vol. 6, p. V006T06A002, 2020.
- [42] S. Kannan, R. Vezhavendhan, S. Kishore and K. V. Kanumuru, "Investigating the effect of orientation, infill density with Triple raster pattern on the tensile properties for 3D Printed samples," *IOPSciNotes*, vol. 1, p. 024405, 2020.
- [43] B. W. Kaplun, R. Zhou, K. W. Jones, M. L. Dunn and C. M. Yakacki, "Influence of orientation on mechanical properties for high-performance fused filament fabricated ultem 9085 and electro-statically dissipative polyetherketoneketone," *Additive Manufacturing*, vol. 36, p. 101527, 2020.
- [44] O. A. Mohamed, S. H. Masood and J. L. Bhowmik. "Optimization of fused deposition modeling process parameters: A review of current research and future prospects," *Advances in Manufacturing*, vol. 3, pp. 42-53, 2015.